AIP | Applied Physics Letters

High efficiency resonance-based spectrum filters with tunable transmission bandwidth fabricated using nanoimprint lithography

Alex F. Kaplan, Ting Xu, and L. Jay Guo

Citation: Appl. Phys. Lett. **99**, 143111 (2011); doi: 10.1063/1.3647633
View online: http://dx.doi.org/10.1063/1.3647633
View Table of Contents: http://apl.aip.org/resource/1/APPLAB/v99/i14
Published by the AIP Publishing LLC.

High efficiency resonance-based spectrum filters with tunable transmission bandwidth fabricated using nanoimprint lithography

Alex F. Kaplan, Ting Xu,[a] and L. Jay Guo[b]
Department of EECS, Center for Nanophotonics and Spintronics, University of Michigan, 1301 Beal Avenue, Ann Arbor, Michigan 48109, USA

(Received 5 August 2011; accepted 15 September 2011; published online 6 October 2011)

We propose a nanostructured color filter based on a metallic resonant waveguide structure capable of extremely high transmission efficiency. As an experimental demonstration, a blue and a red device were fabricated over a large area using nanoimprint lithography. Achieving transmission as high as 90% with a variable transmission bandwidth, these devices exhibit desirable features for numerous color filter applications. © *2011 American Institute of Physics*. [doi:10.1063/1.3647633]

Color filter technology plays a key role for applications in colored displays and image sensors among others. Despite the wide variety of applications, most continue to use colorant-based material to achieve a desired color spectrum, primarily a tri-color package including red, green, and blue (RGB) filters. In recent years, research focus has shifted to thin-film, periodic nanostructures to overcome scaling and durability issues encountered in traditional color filtration.[1–8] For example, perforated metal films[1–4,7,8] and metal-insulator-metal (MIM) structures[5,6] are both capable of filtering a specific spectral band based on the surface plasmon resonance effect. Moreover, perforated metal films that are based on waveguide modes rather than surface plasmons also exhibit spectral filtering effects.[9,10]

Here, we propose and experimentally demonstrate another type of nanostructured color filter based on a metallic resonant waveguide grating (MRWG) structure. Compared with previous reported devices, the peak transmission efficiency of the proposed structure is remarkably improved. Additionally, the design of the MRWG structure also allows for control over transmission bandwidth and the ability to reduce individual filters down to micron-scale pixel sizes. Incident light should be kept close to normal incidence to minimize color variation at larger angles. Apart from various display applications (e.g., near-to-eye displays), these properties can be particularly useful in compact spectrum analysis devices, as well as image sensor technology where high peak transmission is a necessity while scaling and bandwidth control can allow for variations in pixel size and color filter array (CFA) architectures.[11]

The device structure, as shown in Fig. 1(a), consists of two dielectric layers deposited on a glass substrate with a wide linewidth Ag grating on top. Representative transmission spectra for RGB filters are shown in Fig. 1(b). Including the glass substrate, the three dielectrics form a waveguide for the specific frequency band coupled in. The "waveguide" layer is a high index material such as Si_3N_4 while the "buffer" layer is a low index material SiO_2 matched to the glass substrate. To predict the resulting transmission peak wavelength for this structure, we solved the eigenmode equation for the structure formed by the 100 nm-thick "waveguide" layer, the "buffer" layer and substrate. Here, we only consider the transverse magnetic (TM) modes. The permittivity of each layer is assumed to be ε_1, ε_2, and ε_3, respectively, yielding the equation for TM modes as:

$$(k_0^2\varepsilon_1 - \beta^2)^{1/2} d = m\pi + \arctan\left(\frac{\varepsilon_1}{\varepsilon_2}\cdot\frac{\beta^2 - k_0^2\varepsilon_2}{k_0^2\varepsilon_1 - \beta^2}\right)^{1/2} + \arctan\left(\frac{\varepsilon_1}{\varepsilon_3}\cdot\frac{\beta^2 - k_0^2\varepsilon_3}{k_0^2\varepsilon_1 - \beta^2}\right)^{1/2} \quad (1)$$

where β is the propagation constant, k_o is the free space wave number, d is the "waveguide" layer thickness, and m is an integer. The calculated dispersion is shown in Fig. 2, where we can clearly see that the TM_0 mode has a near-linear dispersion across the entire visible spectrum (the shaded region). Since the longitudinal wavevector (i.e., propagation constant β) of the guided modes can be provided by the first order scattering of incident light by the metal grating, given as $\beta = \pm 2\pi/P + k_0 \sin\theta$ (where P is the grating period and θ is the incident angle), we can choose the proper grating period to efficiently couple the incident light into waveguide modes at a specific resonant wavelength. To avoid generating two different resonant modes, here we only consider normal incident light where $\theta = 0$. When propagating along the waveguide layer, the coupled modes will be scattered again by the wide linewidth metal grating. The scattered waves, consequently reflected by the metal grating, will radiate into far field in the forward direction, realizing the spectrum filtering effect at this resonant wavelength. Here, we use COMSOL MULTIPHYSICS simulations to further check the relation between the grating period and the transmission peak wavelength for the proposed structure, as shown in Fig. 2 (marked as green circle). The grating period increases from 250 nm to 450 nm with a step of 10 nm. The grating thickness is 40 nm with a duty-cycle of about 0.75. The thickness of the Si_3N_4 waveguide layer and SiO_2 buffer layer is 100 nm and 50 nm, respectively. Dielectrics were simulated using refractive index values measured from the materials while table values from Ref. 12 were used for metal constants. We can see that

[a]Also at State Key Laboratory of Optical Technologies for Microfabrication, Institute of Optics and Electronics, Chinese Academy of Science, Chengdu, China.
[b]Electronic mail: guo@umich.edu.

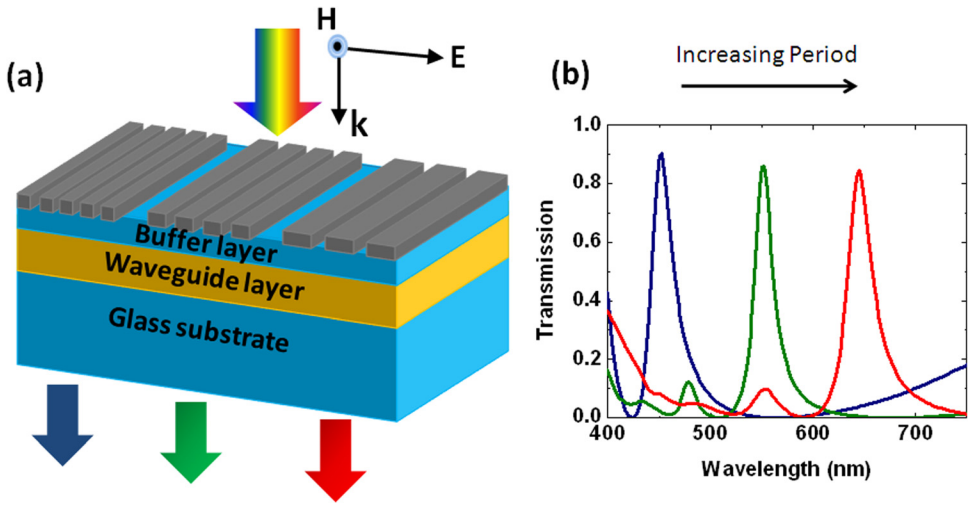

FIG. 1. (Color online) (a) Schematic of the transmissive color filter structure and (b) Simulated transmission spectra

the simulation results agree well with the theoretical calculation, which supports our design based on the MRWG principle.

For the experimental demonstration, we chose grating periods of 280 nm and 420 nm which were available for purchase to realize blue and red color filtering, respectively. In fabrication, both dielectric layers were deposited on a glass substrate using plasma-enhanced chemical vapor deposition (PECVD). The metal layer was fabricated by imprinting a resist (mr-I 8030, Microchem) spun onto the dielectric layers with a wide line width (LW) mold of a defined period using a NX2000 Nanoimprinter (Nanonex, NJ). The residual layer of the resulting narrow LW resist pattern was then etched using an O_2 plasma in a reactive ion etching tool. Ag was then deposited by e-beam evaporation, followed by lift-off in acetone to produce the devices with large duty-cycle Ag grating, as shown in Fig. 3(a).

After fabrication, the transmission spectrum of the device was measured using a Woollam variable angle spectroscopic ellipsometer (WVASE32). Fig. 3(b) shows a comparison between the measured and simulated transmission spectra with TM polarized illumination for the blue (280 nm period) and red (420 nm period) color filters. The measured transmission peak wavelengths (also plotted as red triangles in Fig. 2) are nearly identical with simulated values and high peak transmission is achieved for both filters. The red filter, in particular, matches very well with simulations and achieves ~90% transmission at its peak. The blue filter achieved ~75% peak transmission which is lower than the simulated value. The reason for this, we believe, is mainly due to the defects on the original mold used in the nanoimprint process. Fig. 3(c) shows an SEM image of the 280 nm period metal grating, which contains a large fraction of defects (indicated by arrows) which could decrease transmission significantly for the blue filter. We believe we can reach close to the predicated peak efficiency with future improvements in the initial mold quality. Besides the measured spectrum, the color filtering effect can also be clearly seen from the optical images of the devices illuminated by TM polarized white light, as shown in Figs. 3(d) and 3(e). Here, the size of the color filter we fabricated by nanoimprint lithography is about 1.25 cm × 1.25 cm and the white dots on the images are the defects created from particles in the initial nitride/oxide deposition.

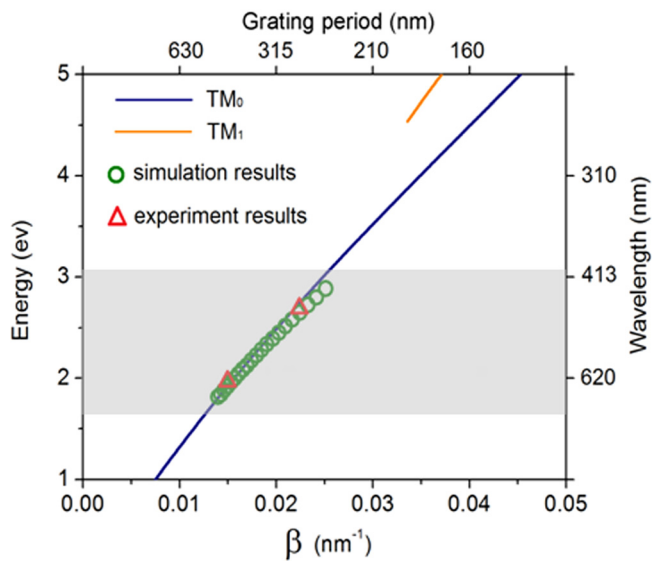

FIG. 2. (Color online) Calculated dispersion of the dielectric waveguide for TM polarized light. The waveguide layer is made of Si_3N_4 with 100 nm-thickness. Surrounding material is SiO_2. Green circles and red triangles correspond to simulation and experiment results, respectively. Shaded region indicates the visible spectrum.

Another distinct advantage of the proposed MRWG filter is that it can be easily tuned from a narrow to a wide bandwidth filter by controlling the "buffer" layer thickness. From the experiment results shown in Fig. 3(b), the full width at half maximum (FWHM) of the transmission band is only about 30 nm, which is much narrower than the previous filters.[1–10] Furthermore, the transmission bandwidth can be controlled by tuning the "buffer" layer thickness. This behavior can be explained by the theory of a metal cladding dielectric waveguide.[13] When the "buffer" layer thickness is reduced, the loss of the waveguide modes from the metal grating will increase, which could decrease the resonance Q factor and result in a wider resonance bandwidth. This effect can be easily seen in Fig. 4, where the FWHM for the fabricated red filter with and without "buffer" layer is about 30 nm and 70 nm, respectively. The ability to tailor the spectral bandwidth could be particularly useful in display and image sensor applications.

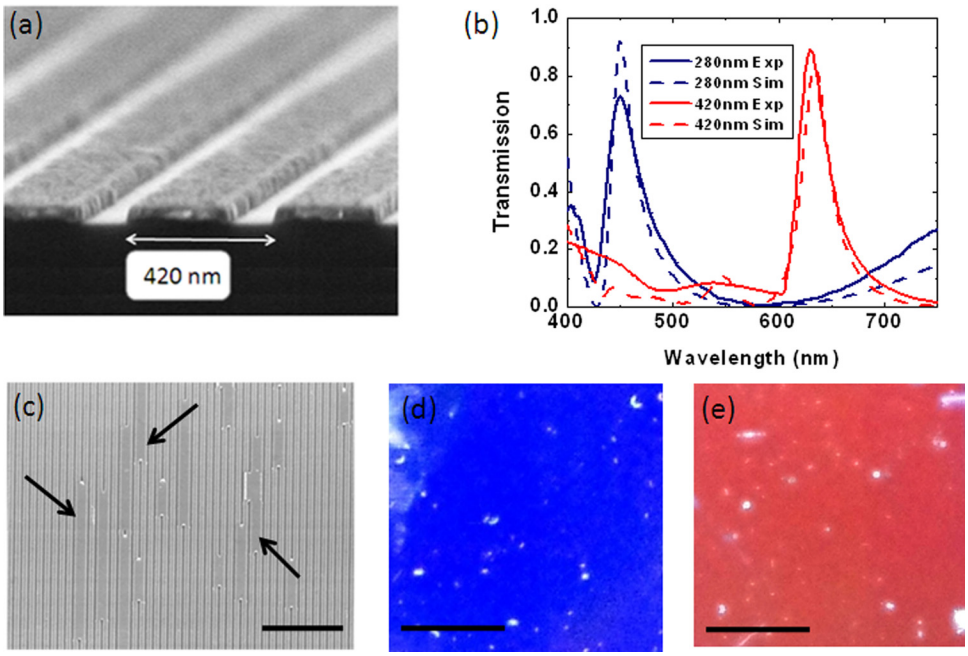

FIG. 3. (Color online) (a) SEM image of the fabricated structure. The grating period is 420 nm. (b) Comparison between experimental and simulated spectra for blue (280 nm period) and red (420 nm period) color filters. (c) SEM image showing defects in 280 nm period metal grating. Scale bar 3 μm. Optical images of (d) blue and (e) red filter illuminated by TM-polarized white light. Scale bar 5 mm.

In summary, we have demonstrated a thin-film color filter device fabricated using nanoimprint lithography with the potential to challenge colorant-based filters in various applications. Fabricated devices demonstrated high transmission peaks with colors controlled by the grating period which matched well with simulated results. The addition of the "buffer" layer thickness provides for specific control over the spectral bandwidth, allowing these filters to be used for a wide variety of devices. Since the structure only requires a single patterning step, it could be fabricated over large areas using roll to roll nanoimprint lithography (R2RNIL)[14,15] or other large area top down processes such as dynamic nanoinscribing.[16,17] Although we only demonstrated a 1D grating structure which works for TM polarized illumination, this design principle can be extended to a 2D structure to achieve polarization-independent color filtering. These filters provide distinct advantages over current color filter technology and could lead to commercial products with greater sensitivity and higher efficiency.

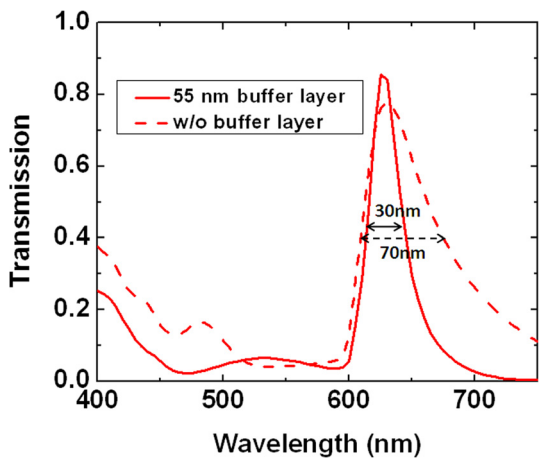

FIG. 4. (Color online) Experimental results demonstrating tunable transmission bandwidth variation for a red (420 nm period) filter with and without oxide "buffer" layer.

The authors acknowledge the support by the University of Michigan ETR fund and by DARPA. The authors Alex Kaplan and Ting Xu contributed equally to this work.

[1]W. L. Barnes, A. Dereux, and T. W. Ebbesen, Nature **424**, 824 (2003).
[2]C. Genet and T. W. Ebbesen, Nature **445**, 39 (2007).
[3]H. S. Lee, Y. T. Yoon, S. S. Lee, S. H. Kim, and K. D. Lee, Opt Express **15**, 15457 (2007).
[4]Y. Ye, H. Zhang, Y. Zhou, and L. Chen, Opt. Commun. **283**, 613 (2010).
[5]T. Xu, Y. K. Wu, X. Luo, and L. J. Guo, Nat. Commun. **1**, 59 (2010).
[6]A. F. Kaplan, T. Xu, Y. K. Wu, and L. J. Guo, J. Vac. Sci. Technol. B **28**, C6O60 (2010).
[7]D. Inoue, A. Miura, T. Nomura, H. Fujikawa, K. Sato, N. Ikeda, D. Tsuya, Y. Sugimoto, and Y. Koide, Appl. Phys. Lett. **98**, 093113 (2011).
[8]N. Nguyen-Huu, Y. L. Lo, and Y. B. Chen, Opt. Commun. **284**, 2473 (2011).
[9]P. B. Catrysse, W. Suh, S. Fan, and M. Peeters, Opt. Lett. **29**, 974 (2004).
[10]C. C. Fesenmaier, Y. Huo, and P. B. Catrysse, Opt. Express **16**, 20457 (2008).
[11]A. E. Gamal and H. Eltoukhy, IEEE Circuits Devices Mag. **21**, 6 (2005).
[12]P. B. Johnson and R. W. Christy, Phys. Rev. B **6**, 4370 (1972).
[13]H. Nishihara, M. Haruna, and T. Suhara, *Optical Integrated Circuits*, (McGraw-Hill, New York, 1989), chap. 2, p. 16.
[14]S. H. Ahn and L. J. Guo, Adv. Mater. **20**, 2044 (2008).
[15]S. H. Ahn and L. J. Guo, ACS Nano **3**, 2304 (2009).
[16]S. H. Ahn and L. J. Guo, Nano Lett. **9**, 4392 (2009).
[17]J. G. Ok, H. J. Park, M. K. Kwak, C. Pina-Hernandez, S. H. Ahn, and L. J. Guo, Adv. Mater. (2011).